

Lamproite dykes in the Napier Complex at Tonagh Island, Enderby Land, East Antarctica

Tomoharu Miyamoto¹, Edward S Grew², John W. Sheraton^{3*},
Martin G. Yates², Daniel J Dunkley^{4**}, Christopher J Carson⁵,
Yasutaka Yoshimura⁶ and Yoichi Motoyoshi⁷

¹*Department of Earth and Planetary Sciences, Kyushu University,
Hakozaki 6-10-1, Fukuoka 812-8581*

²*Department of Geological Sciences, University of Maine,
Orono, Maine 04469-5790, U S A*

³*Department of Geology, Australian National University,
Canberra, ACT 0200, Australia*

⁴*Gamagori Natural History Museum, Minato-cho 17-17,
Gamagori 443-0034*

⁵*Department of Geology and Geophysics, Yale University,
New Haven CT, 06511, U S A*

⁶*Department of Geology, Kochi University, 5-1, Akebono-cho
2-chome, Kochi 780-8520*

⁷*National Institute of Polar Research, Kaga 1-chome,
Itabashi-ku, Tokyo 173-8515*

Abstract: Lamproite dykes, discovered during JARE-40, form NS-trending, subvertical sheets over a 2 km distance in southeastern Tonagh Island. They range from a few centimeters to one meter in thickness and up to several meters in length. The lamproite is holocrystalline and consists dominantly of ferrian microcline, potassic richterite, biotite and apatite, trace amounts of quartz are often present. Grain size is generally 0.1 to 3 mm. The lamproite is noteworthy for its very high contents of K₂O (9.33–11.66 wt%), P₂O₅ (2.66–4.21 wt%), Be (7–19 ppm), F (0.77–1.44 wt%), Rb (253–479 ppm), Sr (2331–3306 ppm), Zr (1310–2400 ppm), Nb (889–209 ppm), Ba (931–12992 ppm), light REE, Th (13–145 ppm) and U (8–16 ppm), and relatively low Al₂O₃ (7.66–10.15 wt%) and Na₂O (1.03–1.95 wt%). Rb-Sr internal isochrons define ages of 466 ± 4 Ma and 476 ± 6 Ma and initial ratios of 0.70949 ± 0.00010 and 0.70966 ± 0.00010, respectively. The small difference in age between the two samples might be related to minor alteration following original crystallization. Lamproites at all three localities have intruded areas where the Archean Napier Complex was reactivated 500 Ma ago by pegmatite activity and by superimposed amphibolite-facies metamorphism and deformation. Overall, the temporal and spatial relationships between lamproite intrusion and zones of late-Proterozoic to Cambrian reactivation of the Napier Complex are similar to those between ultrapotassic igneous activity and

*Present address Stoneacre, Bream Road, St Briavels, Lydney, Glos GL15 6TL, U K

**Present address Division of Geology and Geophysics, School of Geosciences, University of Sydney, NSW 2006, Australia

Pan African deformation and metamorphism in Eastern Queen Maud Land
This suggests that the effects of the amalgamation of east and west Gondwana
extended eastward in Antarctica from Queen Maud Land to Enderby Land

key words lamproite, Enderby Land, Rb-Sr geochronology, magma origin, Pan
African

1. Introduction

Since 1996 the Japanese Antarctic Research Expedition (JARE) has been carrying out the project "SEAL" (Structure and Evolution of east Antarctic Lithosphere), which is an investigation of the geology of the Napier Complex in Enderby Land with the overall aim of understanding the crustal evolution of the Precambrian shield of East Antarctica. For this purpose, field parties of JARE-38 and -39 carried out detailed geological surveys of Mount Riiser-Larsen and Tonagh Island (Ishizuka *et al*, 1998, Osana *et al*, 1999). During a geological survey by JARE-40, dykes of lamproite (as defined by Foley *et al*, 1987, Mitchell and Bergman, 1991, Rock, 1991, Foley, 1992, Woolley *et al*, 1996) were discovered in the southeastern part of Tonagh Island in Amundsen Bay.

Elsewhere in Enderby Land, lamproite dykes have been described from Priestley Peak and from the Hydrographer Islands, respectively, 5 km south and 70 km southwest of Tonagh Island. Field relationships and geochronological data show that these lamproites are unmetamorphosed igneous rocks post-dating the Archean metamorphism of the Napier Complex. The Priestley Peak dyke cuts the youngest, unmetamorphosed mafic dykes (Amundsen dykes) and consists primarily of potassic magnesio-arfvedsonite, biotite, ferrian microcline, apatite, quartz, and minor rutile, titanite and barite (Sheraton and England, 1980, Sheraton *et al*, 1987). A Rb-Sr isochron of whole-rock and mineral samples from this dyke gave an age of 482 ± 3 Ma and an initial ratio of 0.70852 ± 0.00007 (Black and James, 1983). Dykes on the Hydrographer Islands contain richterite, aegirine-augite and barite, and cut shear zones and late (Cambrian) pegmatite, but these dykes have not been dated (Sandiford and Wilson, 1983, 1986).

In general, potassic and ultrapotassic magmas occur in a wide range of tectonic settings, and several models have been proposed for their genesis on the basis of trace element and isotope geochemistry (*eg*, Foley *et al*, 1987, Foley, 1992, Robert *et al*, 1992). Sheraton *et al* (1987) suggested that emplacement of lamproites in Enderby Land and the southern Prince Charles Mountains was associated with faulting which was an early manifestation of the rifting processes that ultimately resulted in the break up of Gondwana.

We report here petrographic and geochemical characteristics of lamproite dykes from Tonagh Island, compare our results with the compositions of other potassic and ultrapotassic rocks, and suggest a tectonic model.

2. Geological setting

Bedrock exposures in Enderby Land consist primarily of high-grade metamorphic rocks. Kamenev (1972, 1975) distinguished the Napier Complex from the Rayner Com-

plex on the basis of its higher metamorphic grade, and inferred that the higher-grade Napier Complex was older than the lower-grade Rayner Complex. This sequence has been confirmed by subsequent geochronological studies (*e.g.*, Williams *et al.*, 1984; Black and James, 1983, Black *et al.*, 1983; Sheraton *et al.*, 1987, Tainosho *et al.*, 1997), which indicate that the Napier Complex is Archean crust 2.5–3.0 Ga in age (with some components as old as 3.8 Ga), whereas the Rayner Complex was metamorphosed at 1.0 Ga and later (*e.g.*, Black *et al.*, 1987). In addition, Sheraton *et al.* (1980, 1987) observed that the unmetamorphosed Amundsen (dolerite) dykes intersect the Napier Complex, whereas the Rayner Complex contains only the metamorphosed relics of such dykes, they also distinguished the complexes on this basis. The dykes, which range in age from 2.35 to 1.20 Ga, constitute part of a Proterozoic igneous province extending over much of southern Africa and parts of formerly contiguous parts of East Antarctica (Sheraton and Black, 1981, Hanson *et al.*, 1998). Localized pegmatites of late Proterozoic or early Cambrian age emplace the Napier and Rayner Complexes (*e.g.*, Grew, 1978, Black *et al.*, 1983, 1987, Sheraton *et al.*, 1987).

Tonagh Island is underlain by granulite-facies metamorphic rocks such as orthopyroxene-bearing felsic orthogneiss, paragneiss, and mafic granulite of the Napier Complex. They are cut by several suites of mafic intrusive rocks, both metamorphosed and unmetamorphosed. Tonagh Island and nearby exposures in Amundsen Bay lie within the area of highest metamorphic grade, and mineral assemblages and textures indicate ultra-high temperature (UHT) conditions (Harley and Hensen, 1990). Osanaï *et al.* (1999) divided the UHT metamorphic rocks of Tonagh Island into five NW-dipping lithologic and structural units (I to V) that are bounded by thrust-shear zones associated with remarkable anhydrous mylonite and later pseudotachylite-cataclasite.

Lamproite dykes are NS-trending, subvertical thin sheets which crop out in the southeast part of Tonagh Island (Fig. 1). Scattered outcrops and float could be followed in a north-south direction for 0.4 km, more float was found 1.4 km further north. Individual bodies range from a few centimeters to one meter in thickness and up to several meters in length (Fig. 2a). The sheets cut the NE-trending gneissosity in the host rock at high angles and are finer grained at their contacts. At locality EG99011413 (Fig. 1), a 1.5 cm thick vein of lamproite has metasomatized the host orthopyroxene-plagioclase granulite in a zone from 3 to 7 mm thick where bundles of richterite have totally replaced orthopyroxene and an unidentified platy to plumose phase has partially replaced plagioclase. Other metasomatic minerals are green aegirine-augite and K-feldspar, some of which shows tartan twinning (microcline), zoning or anomalous interference colors (Fig. 2b).

3. Petrology and mineralogy

The lamproite is holocrystalline and ranges from medium to dark green. Texturally, it is highly variable, some hand specimens contain spangles of biotite, others have centimeter scale layering defined by variations in grain size and proportion of minerals. Biotite grains up to 2 cm, feldspar megacrysts and autoliths up to 1.5 cm × 3 cm are present locally.

The lamproite consists dominantly of microcline, potassic richterite and apatite, and grain size is mostly between 0.1 and 3 mm (Fig. 2c). Biotite is a major constituent in some specimens and is present in all (Fig. 2d), trace amounts of quartz are present in most

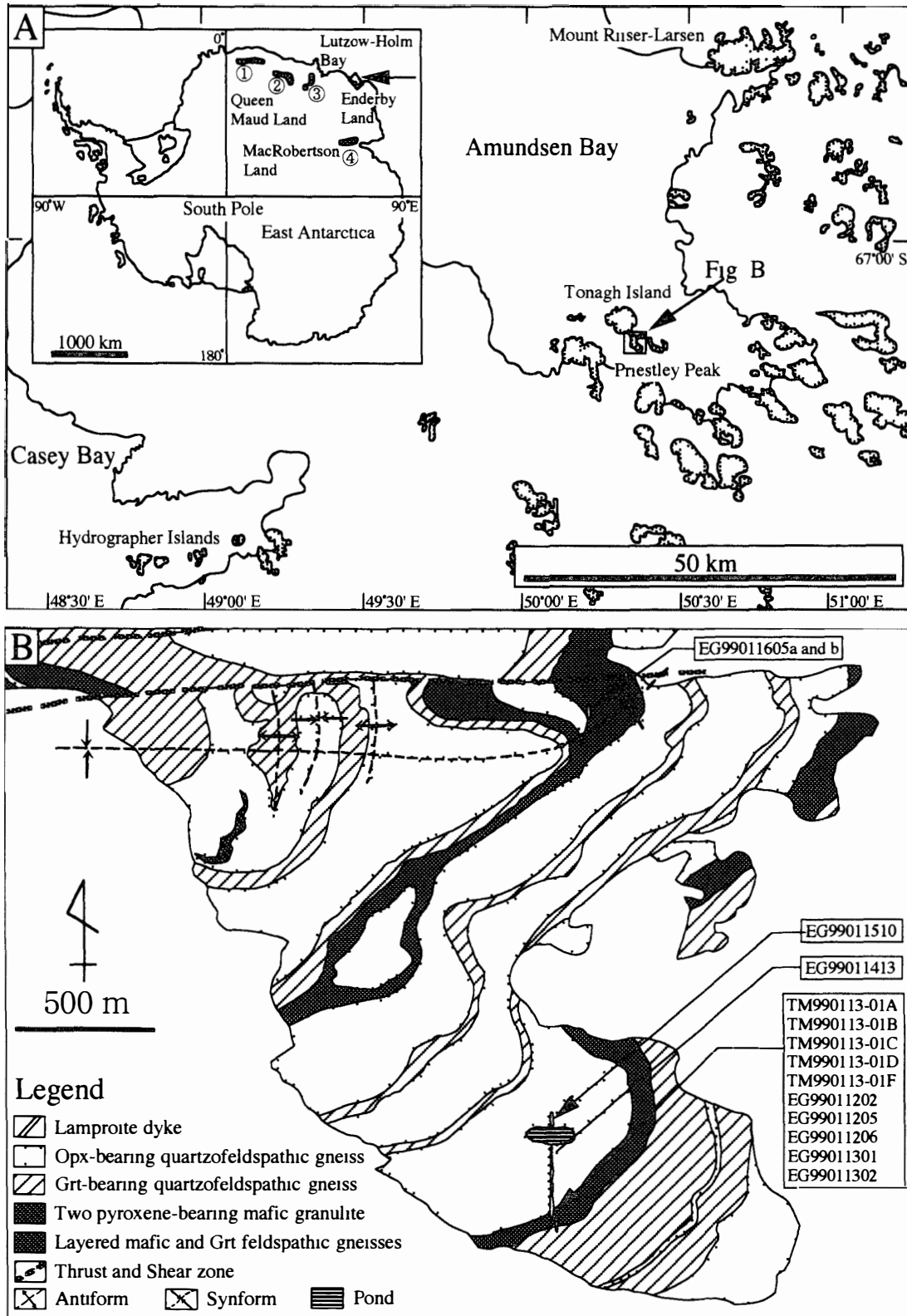


Fig 1 Location map and geological map of Tonagh Island A Location map of Tonagh Island in the western Enderby Land, East Antarctica ① Schirmacher Hills, ② Sør Rondane Mountains, ③ Yamato-Belgica Complex, and ④ Prince Charles Mountains B Geological map of southern Tonagh Island (modified after Osanai *et al*, 1999) showing locality of lamproite dykes

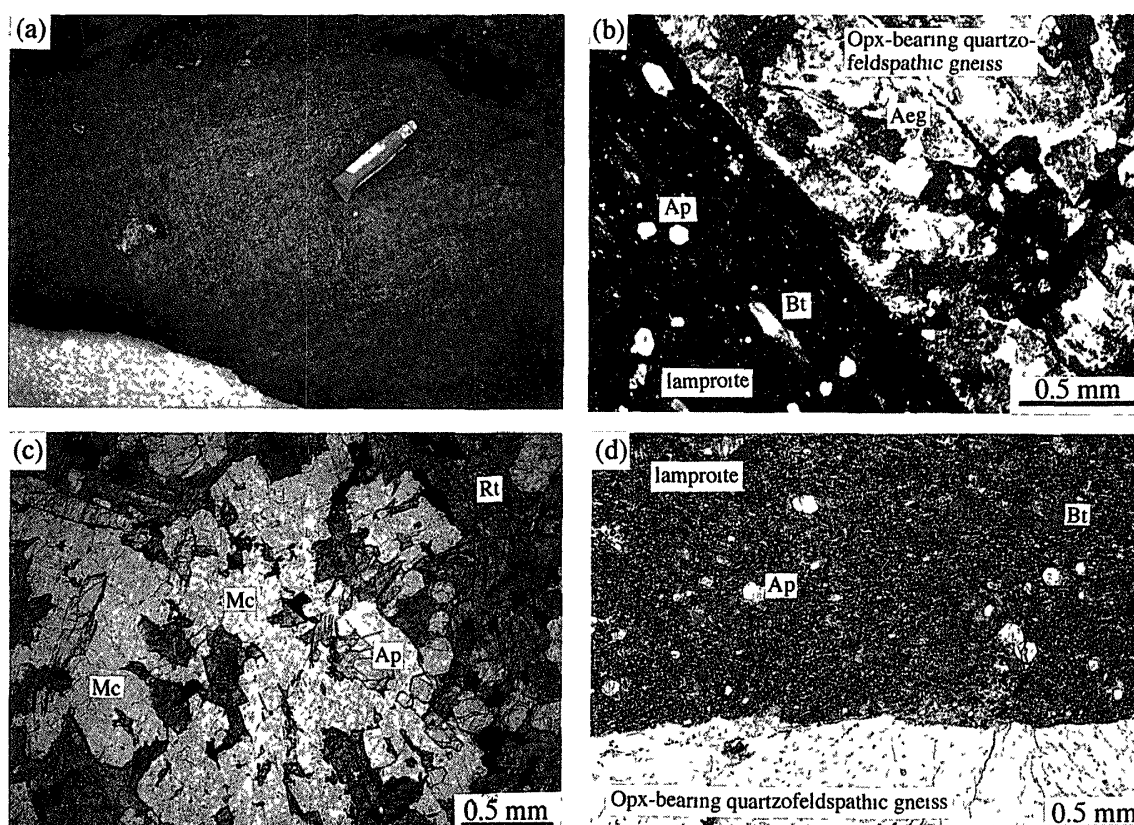


Fig 2 Lamproite from southeast part of Tonagh Island (a) Close up of lamproite dyke in felsic gneiss (b) Photomicrograph of the secondary aegirine-augite in the host orthopyroxene-plagioclase granulite near a vein of the lamproite (EG99011413) Plane polarized light (c) Photomicrograph of biotite-poor lamproite (TM990113-01F) Plane polarized light (d) Photomicrograph of margin of biotite-bearing lamproite (TM990113-01D) with host quartzofeldspathic gneiss Plane polarized light Aeg aegirine-augite, Ap apatite, Bt biotite, Mc microcline, Rt richterite

Rounded titanite and small rutile grains are relatively abundant. Carbonate, zircon and monazite also occur as accessory minerals. Microcline grains typically show the characteristic tartan twinning as well as fine zoning and anomalous interference colors, the last is probably due to the relatively high Fe_2O_3 content (see below). Subhedral biotite, potassic richterite and apatite grains are surrounded by small microcline grains. Fine dusty inclusions are present in the cores of potassic richterite. Some biotite crystals are mantled by potassic richterite coronas. Potassic richterite and microcline become finer-grained toward the margins of the lamproite dykes, whereas biotite and apatite do not (Fig 2d). Autoliths consist largely of the same minerals as the host dyke rock, but are coarser grained, barite is present in one such autolith (sample EG99011605B). Minerals characteristic of many other lamproites, such as Al-poor diopside, leucite, K-Ba-Ti oxides and K-Ti-Zr silicates (Mitchell and Bergman, 1991) were not found, whereas the minerals cited by Mitchell and Bergman (1991) as characteristically absent in lamproites overall were not found in the Tonagh Island lamproite.

Chemical compositions of constituent minerals were determined using a scanning electron microscope (JEOL JSM-5800LV) with an energy dispersive X-ray analytical

Table 1 Average composition of biotite (a), potassic richterite (b) and alkali feldspar (c) from biotite-bearing lamproite (TM990113-01A) and biotite-poor lamproite (TM990113-01F) from Tonagh Island. The parentheses show the number of analyzed grains for each sample.

(a) Biotite					(b) Potassic richterite				
	TM990113-01A		TM990113-01F			TM990113-01A		TM990113-01F	
	Mean (9)	Std Dev	Mean (3)	Std Dev		Mean (14)	Std Dev	Mean (16)	Std Dev
wt%					wt%				
SiO ₂	43.02	0.76	44.34	0.22	SiO ₂	55.53	0.64	55.08	0.64
TiO ₂	2.80	0.35	3.70	0.11	TiO ₂	0.33	0.29	0.38	0.29
Al ₂ O ₃	8.77	0.25	5.54	0.23	Al ₂ O ₃	0.24	0.17	0.08	0.08
Cr ₂ O ₃	0.22	0.23	0.54	0.08	Cr ₂ O ₃	0.16	0.16	0.01	0.01
FeO	14.58	0.97	16.28	0.36	FeO	12.18	0.49	12.56	0.59
MnO	0.16	0.07	0.09	0.02	MnO	0.29	0.09	0.24	0.14
MgO	16.09	0.33	15.35	0.14	MgO	15.73	0.33	15.29	0.54
Na ₂ O	0.65	0.36	0.62	0.09	CaO	4.25	0.18	3.12	0.41
K ₂ O	10.31	0.15	10.18	0.13	Na ₂ O	5.08	0.13	5.47	0.39
Total	96.60		96.64		K ₂ O	3.97	0.29	5.04	0.24
					Total	97.76		97.27	
Cations (O=22)			(O=22) †		Cations (O=23)			(O=23)	
Si	6.324	0.112	6.569	0.032	Si	8.069	0.093	8.097	0.095
Ti	0.309	0.038	0.412	0.012	Ti	0.036	0.031	0.042	0.032
Al	1.519	0.043	0.967	0.040	Al	0.041	0.029	0.015	0.015
Cr	0.025	0.026	0.063	0.010	Cr	0.018	0.018	0.002	0.002
Fe ²⁺	1.792	0.119	2.017	0.045	Fe ²⁺	1.480	0.060	1.544	0.072
Mn	0.020	0.009	0.012	0.003	Mn	0.036	0.012	0.030	0.017
Mg	3.525	0.073	3.391	0.032	Mg	3.408	0.071	3.350	0.119
K	1.933	0.028	1.925	0.025	Ca	0.662	0.027	0.491	0.065
Na	0.184	0.101	0.178	0.026	Na	1.430	0.036	1.560	0.111
Total	15.631		15.534		K	0.736	0.054	0.946	0.044
					Total	15.916		16.077	
(c) Alkali feldspar									
	TM990113-01A		TM990113-01F						
	Mean (12)	Std Dev	Mean (20)	Std Dev					
wt%									
SiO ₂	64.55	0.42	63.84	0.53					
Al ₂ O ₃	16.09	0.70	15.60	0.49					
Fe ₂ O ₃	2.54	0.76	3.22	0.71					
CaO	0.04	0.04	0.02	0.02					
Na ₂ O	0.80	0.04	0.46	0.04					
K ₂ O	16.43	0.22	16.46	0.11					
Total	100.45		99.60						
Cations (O=8)			(O=8)						
Si	3.004	0.020	3.004	0.025					
Al	0.882	0.038	0.865	0.027					
Fe ³⁺	0.089	0.027	0.114	0.025					
Ca	0.002	0.002	0.001	0.001					
Na	0.072	0.003	0.042	0.004					
K	0.975	0.013	0.988	0.007					
Cation	5.024		5.014						

system (OXFORD Link ISIS) at Kyushu University. Representative analyses of the constituent minerals are listed in Table 1. Minerals in metasomatized granulite (Table 2) were analyzed by MGY at the University of Maine; analysis methods are given in Grew *et al.* (2000).

The peralkaline composition of the rock (see below) is reflected in the low Al_2O_3 contents of potassic richterite, biotite and microcline (Table 1). The amphibole is largely potassic richterite ($\text{Ca} > 0.5$ per formula unit), but some analyses give $\text{Ca} < 0.5$ per formula unit such that the average composition for TM990113-01F corresponds to potassic magnesio-arfvedsonite. Metasomatic richterite is more calcic; it is noteworthy for its relatively high F content (Table 2). Excess Si_1 in the amphibole, that is, $\text{Si}_1 > 8$ per formula unit, could result from assuming that all Fe is divalent when actually a substantial proportion is ferric. Metasomatic aegirine-augite is close to 50% aegirine, 25% diopside,

Table 2 Selected analyses of metasomatic minerals in sample EG99011413

	Aegirine-augite	Richterite	Microcline
wt %			
SiO_2	52.52	55.01	65.64
TiO_2	0.29	0.14	0.00
Al_2O_3	0.14	0.53	17.83
Fe_2O_3	16.00	-	0.75
FeO	8.49	11.30	-
MnO	0.36	0.33	0.00
MgO	4.14	16.62	0.00
CaO	9.86	9.33	0.00
Na_2O	7.38	2.04	0.63
K_2O	0.00	1.05	16.13
F	-	1.48	-
Cl	-	0.00	-
H_2O	-	1.36	-
O=F, Cl	-	-0.62	-
Total	99.18	98.57	100.98
Cations	(O=6)	(O=23)	(O=8)
Si	2.032	7.991	3.013
Ti	0.009	0.015	0.000
Al	0.006	0.091	0.965
Fe^{3+}	0.466	-	0.026
Fe^{2+}	0.275	1.373	-
Mn	0.012	0.041	0.000
Mg	0.239	3.600	0.000
Ca	0.409	1.452	0.000
Na	0.553	0.575	0.056
K	0.000	0.195	0.944
Total cations	4.000	15.333	5.004
Anions			
F	-	0.681	-
Cl	-	0.000	-
OH	-	1.319	-
Total anions	-	2.000	-

* $\text{Fe}_2\text{O}_3/\text{FeO}$ ratio of aegirine-augite was calculated assuming O=6 and sum cations=4. For richterite, all Fe assumed to be FeO and H_2O calculated from $\text{F} + \text{Cl} + \text{OH} = 2$. For microcline, all Fe assumed to be Fe_2O_3 .

and 25% hedenbergite in composition. The presence of tetrahedral Fe^{3+} in biotite is suggested by the deficiency in total tetrahedral cations ($\text{Si}_1 + \text{Al} < 8$ per formula unit). Its presence is more certain in microcline, both igneous (Table 1) and metasomatic (Table 2), in which up to 0.114 Fe^{3+} substitutes for Al. Anomalous interference colors could be characteristic of ferric microcline, Grew *et al* (1994) reported such anomalous colors in a metamorphic K-feldspar containing 0.084–0.222 Fe^{3+} per formula unit.

The microcline in lamproite from Tonagh Island has a higher Fe_2O_3 than most alkali feldspar except sanidine in volcanic rocks (*e.g.*, Deer *et al*, 1963). Smith (1974) suggested that the Fe content of alkali feldspars correlates with the temperature of equilibration, and that Fe would be expelled from the feldspar during slow cooling. Possibly the cooling rate of the lamproite was sufficiently rapid for alkali feldspar which originally crystallized as ferric sanidine and then inverted to microcline did not expel Fe.

The titanium-rich composition of the rock is reflected in the relatively high TiO_2 contents of biotite. However, potassic richterite and potassic arfvedsonite contain much less TiO_2 than the 2–9 wt% typical of lamproite amphiboles (Mitchell and Bergman, 1991). It is possible that amphiboles in the Tonagh Island lamproite were depleted in Ti during cooling when sanidine inverted to microcline, and the Ti released thereby was incorporated in rutile and titanite.

4. Geochemistry

Whole rock compositions of the five samples collected by TM (TM990113–01A, B, C, D and F) were determined by X-ray fluorescence spectrometry (XRF; Rigaku-GF3063P) at Kyushu University. Whole rock compositions of eight samples collected by ESG (prefix EG9901-) were determined by the following methods at the Australian National University: (1) XRF using glass discs—Si, Ti, Al, total Fe, Mn, Mg, Ca, Na, K, P, S, Cl, (2) XRF using pressed powders—Y, Zr, Nb, Cs, Hf, Ta, La, Ce, Pr, Nd, Th, U, Sc, V, Ni, Cu, Zn, Ga, Ge, As, Se, Br, Nb, Mo, Ag, Cd, In, Sn, Sb, Te, I, Tl, Pb, Bi, Cr, Rb, Sr, Ba, (3) CO_2 , $\text{H}_2\text{O}(-)$ and $\text{H}_2\text{O}(+)$ were analyzed using a Leco combustion furnace under an N_2 atmosphere, the temperature was increased up to 120°C to determine the $\text{H}_2\text{O}(-)$ and then to 1040°C to obtain the $\text{H}_2\text{O}(+)$ and CO_2 , (4) Fe^{2+} was done by wet chemistry: acid digestion followed by dichromate titration. The remaining elements were measured at Analabs, Perth, Western Australia as follows: (1) inductively coupled plasma mass spectrometry (ICP-MS) for Li, Be, (2) inductively coupled plasma atomic emission spectrometry (ICP-AES) for B, and (3) ion sensitive electrode for F.

Major and trace element compositions of the lamproites are given Tables 3 and 4. The Tonagh Island lamproites are heterogeneous, especially sample EG99011605 (a and b are parts of a larger piece), which differs markedly from the other samples. This sample is finer-grained and contains more biotite than the other samples, part 1605b contains barite. These mineralogical differences are reflected in the substantially higher F, S, Ti, Rb, Ba and Cs, and lower Na and Si, other compositional differences include higher Cr, Ni, Nb and Te, and lower Y.

The Tonagh Island lamproites all have the distinctive chemical features of lamproites in general as summarized by Rock (1991, Table 5.1) and Mitchell and Bergman (1991), *e.g.*, Niggli mg (0.50–0.72), Niggli k (0.76–0.87), molar $\text{K}_2\text{O}/\text{Na}_2\text{O}$ ratio (3.21–6.66) and molar

Table 3 Major elements compositions (wt%) of lamproites from Tonagh Island

	TM9901 13-01A	TM9901 13-01B	TM9901 13-01C	TM9901 13-01D	TM9901 13-01F	EG9901 1202	EG9901 1205	EG9901 1206	EG9901 1301	EG9901 1302	EG9901 1510	EG9901 1605a	EG9901 1605b
SiO ₂	57.53	57.36	55.83	57.40	54.44	53.68	51.09	54.43	54.66	52.79	53.15	47.66	47.74
TiO ₂	1.87	1.93	2.34	2.36	2.40	2.18	2.74	2.14	2.34	2.60	2.50	4.95	4.93
Al ₂ O ₃	9.05	9.15	10.15	9.21	8.21	8.41	8.41	9.26	8.19	7.66	8.88	8.41	8.52
Fe ₂ O ₃ *	6.12	5.86	5.09	5.61	6.40	3.42	2.83	3.18	3.42	3.63	3.24	3.14	3.16
FeO						2.69	2.79	2.08	2.69	3.02	2.60	1.77	1.79
MnO	0.12	0.12	0.10	0.12	0.11	0.13	0.09	0.09	0.10	0.12	0.12	0.07	0.07
MgO	5.21	5.23	5.59	5.35	6.19	6.08	7.22	5.64	5.26	6.10	5.31	8.12	8.09
CaO	5.19	5.36	4.76	5.09	5.48	6.23	6.83	5.75	5.41	5.86	5.85	5.31	5.15
Na ₂ O	1.70	1.71	1.62	1.44	1.93	1.94	1.45	1.81	1.66	1.93	1.34	1.03	1.08
K ₂ O	10.43	10.49	11.66	10.80	10.18	9.44	9.52	10.30	9.56	9.33	9.40	10.45	10.46
P ₂ O ₅	2.87	2.99	2.84	2.82	3.12	2.91	4.21	3.08	2.66	2.83	2.68	3.30	3.29
CO ₂						0.37	0.11	0.26	1.55	1.44	2.21	0.89	0.74
H ₂ O (-)						0.13	0.17	0.19	0.24	0.23	0.31	0.23	0.22
H ₂ O (+)						0.33	0.44	0.32	0.43	0.47	0.62	0.68	0.67
F						1.19	1.29	1.06	0.90	1.05	0.77	1.44	1.33
S						0.01	0.02	0.02	0.03	0.05	0.13	0.38	0.36
O=F, Cl, S						-0.51	-0.56	-0.46	-0.39	-0.47	-0.39	-0.80	-0.74
Total	100.09	100.20	99.96	100.20	98.47	99.65	99.69	100.23	99.74	99.86	100.08	99.58	99.37

*For samples TM990113-01A, B, C, D and F, total iron as Fe₂O₃

K₂O/Al₂O₃ ratio (1.15–1.35) all fit the criteria cited by Mitchell and Bergman (1991) for recognition of lamproite. Noteworthy deviations from the average composition that Rock (1991) gave are even greater enrichment in the Tonagh Island lamproite of K₂O, P₂O₅, F, Cl, Li, and the incompatible elements Sr, Zr, La, Ce, Pr, Pb and U; Na₂O and Y are also higher. However, TiO₂, MgO, H₂O and the compatible trace elements Cr and Ni are lower. Ba is less enriched, except that the TiO₂, Cr, Ni and Ba contents in 1605a and 1605b are closer or exceed the averages cited by Rock (1991). In terms of the CaO-Al₂O₃ diagram of Foley *et al.* (1987) (Fig. 3), the Tonagh Island lamproites plot in the field of Group I lamproites, which have the highest concentrations of incompatible trace elements. A spidergram of primitive mantle normalized incompatible element abundances (Fig. 4) shows negative spikes for Nb-Ta, Sr and P that are characteristic of Group I (Foley *et al.*, 1987). However, depletion in Y is less than for typical Group I ultrapotassic rocks. F concentrations exceed the maximum amounts cited by Foley *et al.* (1986) for Group I (0.8 wt%) and by Rock (1991) for lamproites (0.9 wt%), whereas Cl concentrations are among the higher values cited by Rock (1991).

The Priestley Peak lamproite shows many of the distinctive features noted above for the Tonagh Island lamproite. Although it is not so enriched in Rb, Nb, La, Ce and Pb, it is even more enriched in S and Ba, which is consistent with the presence of 1 modal% barite (Sheraton and England, 1980). The Hydrographer Islands lamproite differs from the Priestley Peak and Tonagh Island lamproites in containing more SiO₂, Al₂O₃ and total Fe oxide but less P₂O₅, Rb, Sr, Zr and Pb, which could explain the presence of aegirine-augite (Sandiford and Wilson, 1983). Lamproites from both localities are rich in Cl, averaging nearly 400 ppm, but no F data were given.

Concentrations of the light lithophile elements Be and B are not often given for

Table 4 Minor elements abundances (ppm) of lamproites from southeastern Tonagh Island

	TM9901 13-01A	TM9901 13-01B	TM9901 13-01C	TM9901 13-01D	TM9901 13-01F	EG9901 1202	EG9901 1205	EG9901 1206	EG9901 1301	EG9901 1302	EG9901 1510	EG9901 1605a	EG9901 1605b
Li						105.5	187	54.1	26.4	35	61.8	24.3	23.1
Be						11.9	12.4	6.6	15.2	18.5	11.4	9.4	10.0
B						30	30	24	20	30	<20	28	26
Cl						264	220	215	117	200	225	319	314
S						136	160	168	264	521	1258	3789	3564
Sc						26	24	26	24	24	24	16	16
V						116	114	68	92	126	76	98	94
Cr	126	111	139	125	207	188	232	158	160	224	138	416	428
Ni						166.4	199.8	144.9	146.2	193.8	120.4	339.3	345.2
Cu						39.6	115.7	49.0	92.1	92.2	78.1	69.0	67.3
Zn						130.9	108.4	89.0	107.5	137	84.3	89.1	87.8
Ga						4.5	14.8	15.6	16.0	11.3	16.8	16.8	15.4
Ge						0.4	0.9	1.8	1.1	1.9	<0.6	<0.6	0.5
As						4.5	2.0	4.2	1.4	2.0	1.0	<0.9	<1
Se						<0.4	<0.3	<0.3	<0.4	0.5	<0.4	0.6	<0.4
Br						1.7	1.4	3.1	1.1	1.9	1.7	0.8	1.8
Rb	321	313	353	363	266	282.5	320.1	297.7	263.5	252.5	280.4	478.7	458.6
Sr	2331	2399	2788	2643	2642	2374	3306	2423	2506	2547	2976	2505	2469
Y	156	158	81.6	111	58.7	77.7	42.1	75.0	39.9	34.3	44.4	18.9	18.0
Zr			1175		1388	1690	1310	1570	1710	1860	2130	2400	2380
Nb	127	112	25.4	82.0	150	91.9	89.0	91.7	112.2	151.1	97.2	198.5	209.1
Mo						0.8	0.9	2.1	1.5	0.7	1.9	4.0	2.4
Ag						0.3	0.3	0.2	<0.1	<0.2	<0.2	<0.3	<0.3
Cd						<0.1	<0.1	<0.2	<0.1	<0.2	<0.2	0.6	0.6
Sn						5.8	4.4	3.4	5.5	5.0	8.7	10.6	10.5
In						<0.2	<0.2	<0.2	<0.2	<0.2	<0.2	1.0	1.1
Sb						<0.1	<0.1	<0.2	<0.1	<0.2	<0.2	2.6	2.5
Te						<0.3	<0.3	<0.3	<0.3	<0.3	<0.3	10.6	9.8
I						<0.5	<0.5	<0.5	<0.6	<0.7	<0.7	<1.8	<1.7
Cs						<0.6	<0.6	<0.7	<0.7	<0.8	<0.9	15.6	13.5
Ba						931	815	1191	1737	2901	3376	13359	12992
La						274	298	510	772	242	286	272	282
Ce						828.1	774.8	1146	625.2	538.9	701.2	599.5	624
Pr						124.2	101.1	152.0	76.8	67.6	101.5	138.3	135.4
Nd						380	325	405	245	225	300	195	195
Hf						49.2	34.0	42.4	41.3	50.9	53.6	59.6	61.9
Ta						4.5	6.1	5.2	5.3	<5	7	9.1	11.9
Tl						1.3	2.3	2.3	1.5	2.0	2.5	1.8	2.7
Pb						400	48	76	92	200	90	66	78
Bi						2.9	1.5	1.4	2.0	2.1	2.3	2.7	2.0
Th						13	13	33	52	26	145	28	69
U						10	13	37	17	14	16	8	8

potassic and ultrapotassic rocks on account of difficulties of their analyses (*e.g.* Sheraton and England, 1980, Thompson and Fowler, 1986, Pognante, 1990, Vaselli and Conticelli, 1990, Arima and Shiraishi, 1993, Kononova *et al.*, 1997, Miller *et al.*, 1999) Rock (1991) reported only six Be and no B analyses for lamproites (*cf.* 524 analyses for Li, 846 analyses overall) and gave an average of 6 ppm Be for lamproite. However, 3–33 ppm Be were reported in West Kimberley, Australia, lamproites (Mitchell and Bergman, 1991) and 9–21 ppm Be in ultrapotassic volcanic rocks in SW Tibet (Miller *et al.*, 1999). Reported B contents are comparable to those reported here: 4–54 ppm B in lamproite and rocks of lamproitic affinity from central Italy (Vaselli and Conticelli, 1990) and 1–31 ppm B in Francis and West Kimberley lamproites (Mitchell and Bergman, 1991). Be is enriched in

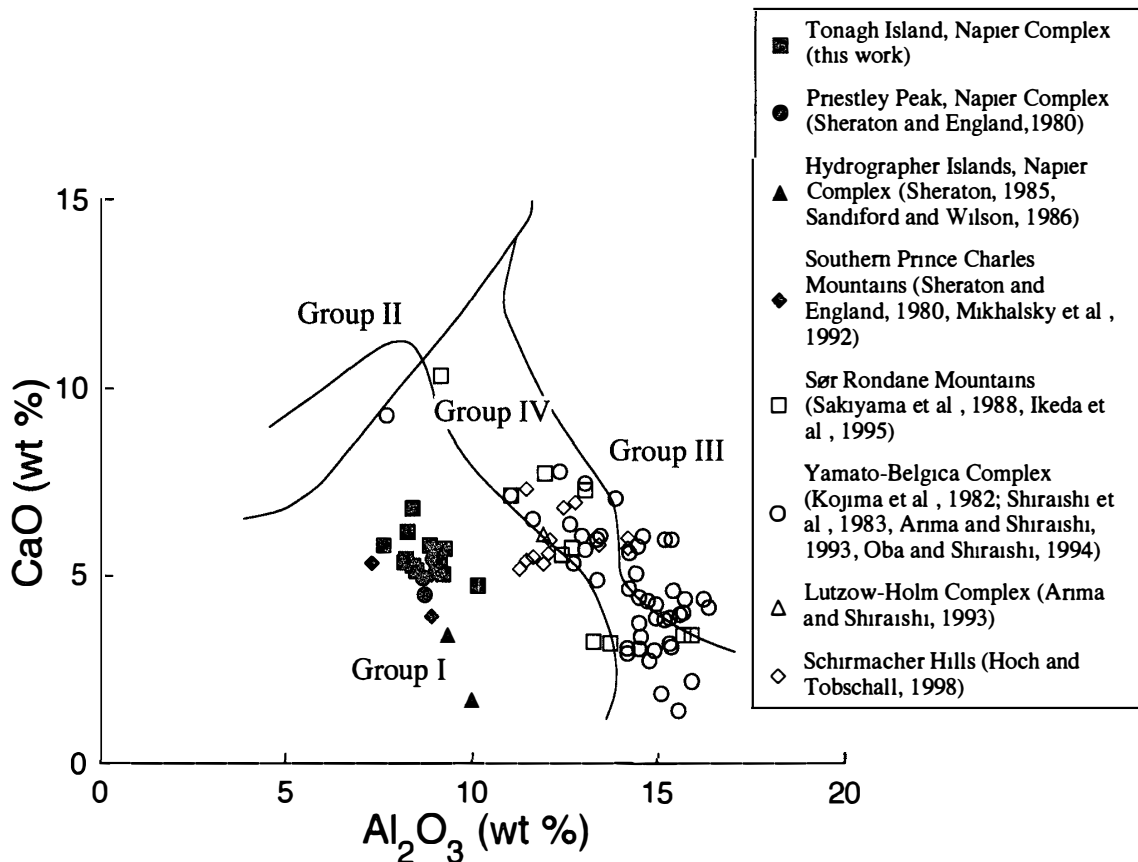


Fig 3 $CaO-Al_2O_3$ discrimination diagram for ultrapotassic igneous rocks after Foley et al (1987). Lamproites from Enderby Land and southern Prince Charles Mountains (solid symbols) are all plotted in the Group I field. Used data are compiled from Sheraton and England (1980), Sheraton (1985), Sandiford and Wilson (1986) and Mikhalsky et al (1992). Potassic and ultrapotassic rocks from Eastern Queen Maud Land (open symbols) are Al-enriched and plotted mainly in the transitional area between Groups I and III (i.e. Group IV) on the same discrimination diagram (Data for Queen Maud Land are compiled from Kojima et al, 1982, Shiraishi et al, 1983, Sakiyama et al, 1988, Arima and Shiraishi, 1993, Oba and Shiraishi, 1994, Ikeda et al, 1995, Hoch and Tobschall, 1998).

the Tonagh Island lamproite by factors, respectively, of 110–308 times the primitive mantle values calculated by Taylor and McLennan (1985), whereas B is enriched by factors not exceeding 50 times these values. That is, enrichment of Be is comparable to that of the less-enriched elements such as Nb, Ta and Zr, whereas enrichment of B is more comparable to that of Y.

5. Geochronology

Potassic richterite, biotite, microcline and apatite were concentrated from two samples of lamproite (TM990113-01A and F). After crushing and the elimination of fine powder with water, the grains were separated into non-magnetic and magnetic fractions by Frantz isodynamic separator. Non-magnetic grains heavier than tetrabromoethene were suspended in methylene iodide and separated into lighter (NM1) and heavier fractions. NM1

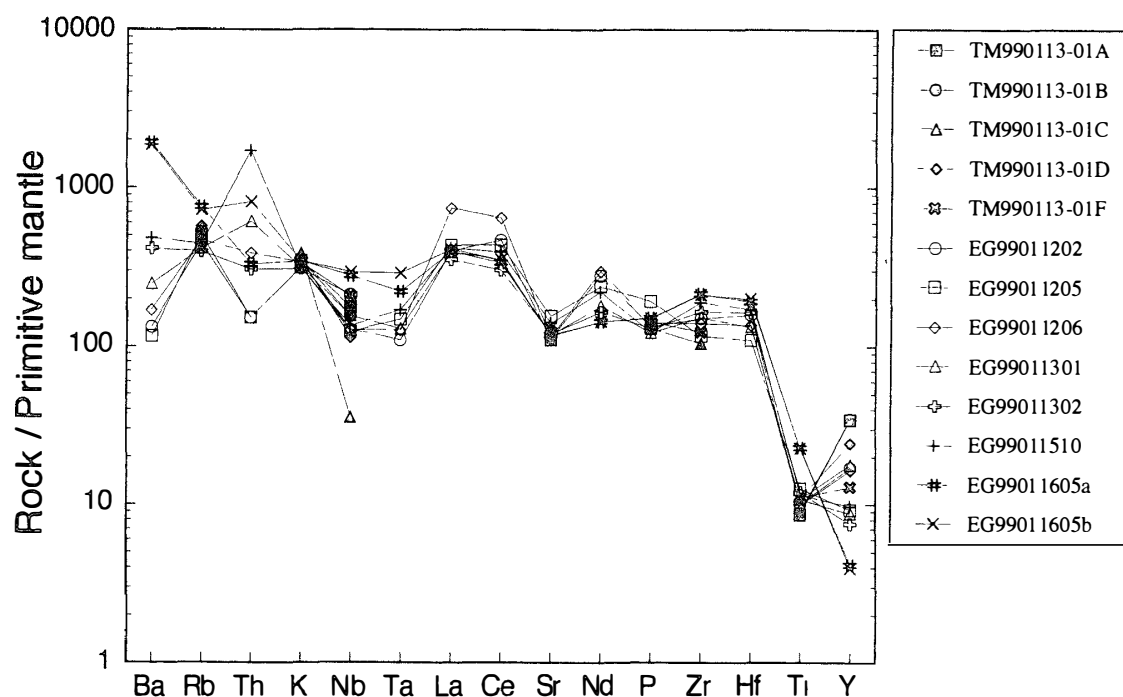


Fig 4 Spidergram for lamproites Estimated primitive mantle abundances from Sun and McDonough (1989)

consists mainly of apatite and the heavier fraction mainly of zircon and monazite. Non-magnetic grains lighter than tetrabromoethene were suspended in a tetrabromoethene-acetone mixture with specific gravity of 2.60 to give the lighter fraction NM2, which consists mainly of microcline. Magnetic grains were sieved to check variation by grain size. Biotite (Bt) and potassic richterite (Rt) fractions were separated from magnetic grains of each size class by magnetic separator and heavy liquids. Complete separation of biotite and potassic richterite was difficult because their magnetic susceptibilities and densities overlapped and because biotite grains are mantled by potassic richterite. Finally, these grains were concentrated and an attempt was made to purify by hand picking under a binocular microscope. These grain separates were analyzed along with the rock sample (WA and WF).

Conventional isotope dilution methods were applied to determine rubidium and strontium contents in the samples (Yanagi *et al*, 1988). The barium coprecipitation method was employed for separation of strontium. Rubidium concentration was determined with a HITACHI RMU5G mass spectrometer, whereas strontium isotope composition and total Sr abundance were determined with JEOL JMS05RB mass spectrometer by measuring the isotope compositions of spiked samples (Yanagi, 1990). The strontium standard of Eimer and Amend gave the values of $^{87}\text{Sr}/^{86}\text{Sr} = 0.7080 \pm 0.0001$ (1σ) in this study. The decay constant for ^{87}Rb used is $1.42 \times 10^{-11} \text{ year}^{-1}$ (Steiger and Jager, 1977).

Rb-Sr analytical data on mineral concentrates and whole rock samples are listed in Table 5. Internal Rb-Sr isochrons determined from lamproite samples TM990113-01A and -01F by the least squares regression method (York, 1966) gave, respectively, ages of $466 \pm 4 \text{ Ma}$ (Fig 5) and of $476 \pm 6 \text{ Ma}$ (Fig 6) together with initial ratios of 0.70949 ± 0.00010 and 0.70966 ± 0.00010 . The small difference in ages between the two samples

Table 5 Analytical data for whole rock and mineral concentrates of lamproites TM990113-01A and TM990113-01F from southeastern Tonagh Island

	Rb (ppm)	Sr (ppm)	$^{87}\text{Rb}/^{86}\text{Sr}$	$^{87}\text{Sr}/^{86}\text{Sr}$
<i>TM990113-01A</i>				
Whole Rock (WA)	322	2331	0.4000	0.71227 ± 7
Biotite				
0.50 < 2R < 0.71 mm (Bt1)	693	290	6.956	0.75541 ± 7
0.35 < 2R < 0.50 mm (Bt2)	717	163	12.86	0.79512 ± 18
0.25 < 2R < 0.35 mm (Bt3)	637	467	3.956	0.73555 ± 6
Richtente				
0.35 < 2R < 0.50 mm (Rt2)	323	1222	0.7645	0.71471 ± 14
0.25 < 2R < 0.35 mm (Rt3)	256	1340	0.5534	0.71320 ± 10
Non-magnetic fraction				
2.96 < ρ < 3.33 (NM1)	105	9319	0.03250	0.70971 ± 10
ρ = 2.60 (NM2)	480	324	4.295	0.73660 ± 10
<i>TM990113-01F</i>				
Whole Rock (WF)	266	2642	0.2910	0.71159 ± 6
Biotite				
0.50 < 2R < 0.71 mm (Bt1)	669	781	2.484	0.72651 ± 21
0.35 < 2R < 0.50 mm (Bt2)	670	701	2.772	0.72851 ± 14
0.25 < 2R < 0.35 mm (Bt3)	660	112	17.27	0.82697 ± 24
Richtente				
0.50 < 2R < 0.71 mm (Rt1)	288	1932	0.4320	0.71273 ± 8
0.35 < 2R < 0.50 mm (Rt2)	274	1976	0.4022	0.71248 ± 5
0.25 < 2R < 0.35 mm (Rt3)	114	2597	0.1277	0.71042 ± 27
Non-magnetic fraction				
ρ = 2.60 (NM2)	495	394	3.641	0.73412 ± 9

*Errors given are ± 1σ

R indicates the radius of grains, ρ indicates the gravity of fractions

Relative analytical errors in Rb and Sr concentrations are under 2% and 1%, respectively

might be related to minor alteration during annealing that disrupted the isotopic system in mineral phases following original crystallization. Thus, the isochron for TM990113-01A might date the age of this later alteration instead of original crystallization. The internal isochron age of sample TM990113-01F is very close to the 482 ± 3 Ma age reported by Black and James (1983), but the latter authors calculated an initial ratio of 0.70852 ± 0.00007 . Consequently, the lamproites at Tonagh Island and Priestley Peak can be regarded as contemporaneous, although the difference in initial ratios suggests that their sources might not have been identical.

6. Discussion and comparisons

The chemistry of lamproites can serve as indicators of the tectonic regimes at the time

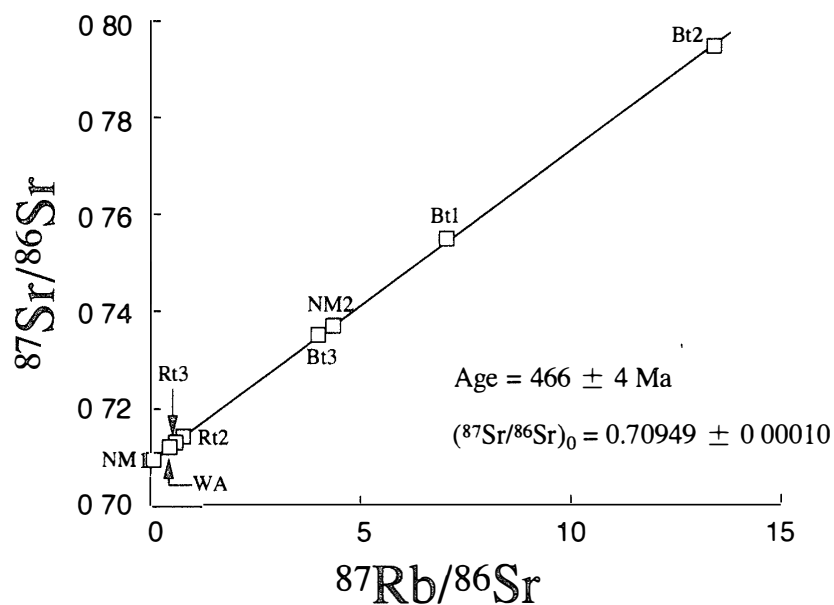


Fig 5 Rb-Sr isochron diagram for whole rock and mineral fractions from lamproite sample TM990113-01A. Errors given are $\pm 1\sigma$. Letters and numbers identifying the points refer to the sample fractions in Table 5.

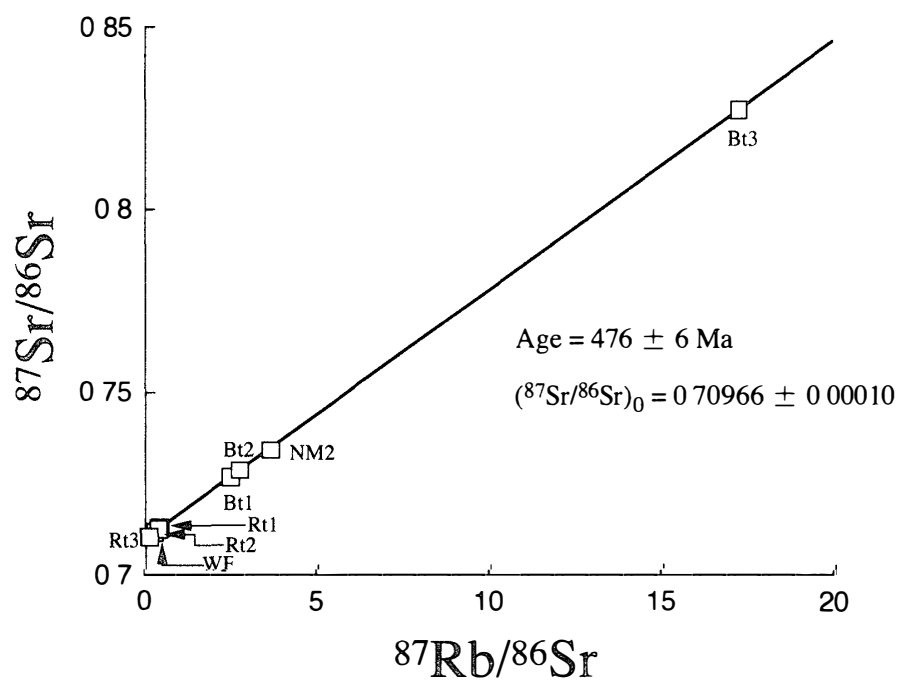


Fig 6 Rb-Sr isochron diagram for whole rock and mineral fractions from lamproite sample TM990113-01F. Errors given are $\pm 1\sigma$. Letters and numbers identifying the points refer to the sample fractions in Table 5.

of emplacement. In general, lamproites are characteristic of intraplate igneous activity in either old stable cratons or recently stabilized ones (*e.g.*, Mitchell and Bergman, 1991, Rock, 1991). In Enderby Land, lamproites have been found only in southern Amundsen Bay and western Casey Bay, two areas of the Napier Complex with relatively abundant intrusions of late pegmatites (*e.g.*, Sheraton *et al.*, 1987), one of which was dated as early Cambrian (522 Ma; Black *et al.*, 1983). Several such late pegmatites, which contain beryl, tourmaline and muscovite, were discovered on Tonagh Island during field surveys by JARE-40 (E S Grew, unpublished data). In addition, western Casey Bay was affected by intense superimposed metamorphism and deformation at about 500 Ma (Black *et al.*, 1983, Sandiford and Wilson, 1983). This spatial association of lamproites and other post-Archean activity suggests that the zones of reactivation formed 500 Ma ago in the Napier Complex were zones of weakness favored by post-reactivation intrusion of lamproite.

It is unlikely that the Enderby Land lamproites are primary magmas given that their SiO₂ contents exceed 50 wt%, Cr and Ni concentrations do not exceed 1000 and 500 ppm, respectively, and mantle xenoliths are absent (Foley *et al.*, 1987). More likely, their compositions resulted from fractionation. Details of lamproite geochemistry could shed light on whether there is subducted lithosphere under the Napier Complex, that is, in the present case whether the Napier Complex was near an active continental margin during reactivation 520 Ma ago. The presence of a subducted component in the mantle source of the lamproites could have left a trace element or isotopic signatures in the lamproites emplaced 40 Ma afterward. Trace element data for the Napier Complex lamproites give conflicting evidence on the nature of the mantle source. For example, lamproites from Amundsen Bay plot in the field of within-plate rocks in terms of TiO₂ and Al₂O₃ (Müller *et al.*, 1992), whereas the Hydrographer Island lamproite plots near the boundary with arc-related rocks (Fig 7). Nb concentrations give even more conflicting results. The high Nb contents of Tonagh Island lamproite (mostly > 100 ppm) are characteristic of areas remote from subduction, whereas the lower Nb contents of the Priestley Peak rocks (50 ppm) plot near the field for areas closely related to subduction in space or time (Thompson and Fowler, 1986). Miller *et al.* (1999) and Ben Othman *et al.* (1989) cited several trace element ratios diagnostic of subducted sediment. Ce/Pb, Sr/Nd and Nb/La ratios would be lower in sediment than oceanic basalts, whereas Cs/Rb, Th/Ta and Th/La ratios would be higher. Most of the ratios measured in the Tonagh Island and Priestley Peak lamproite have values consistent with an absence of sedimentary components, but Nb/La and Ce/Sr ratios could indicate a sedimentary component (the relevant trace element data are not available for the Hydrographer Islands). The negative anomalies for Ta, Nb and Ti on the spidergram (Fig. 4) could indicate a subduction setting, but Rock (1991) opined that attaching any clear genetic significance to these anomalies was still premature; Müller *et al.* (1992) concluded that these anomalies were not diagnostic. In summary, Sm-Nd and Pb isotope data would be needed for a more definitive discussion of the origin of the Enderby Land lamproites.

Elsewhere in Antarctica, lamproites in dykes at Mount Bayliss (Sheraton and England, 1980) and in Mount Rubin (Mikhalsky *et al.*, 1992, 1994) in the southern Prince Charles Mountains, MacRobertson Land are probably the ultrapotassic rock most similar to the Enderby Land lamproites. The presence of possible pseudoleucite in a much finer grained sample from moraine at the Mount Bayliss and Mount Rubin dyke suggests

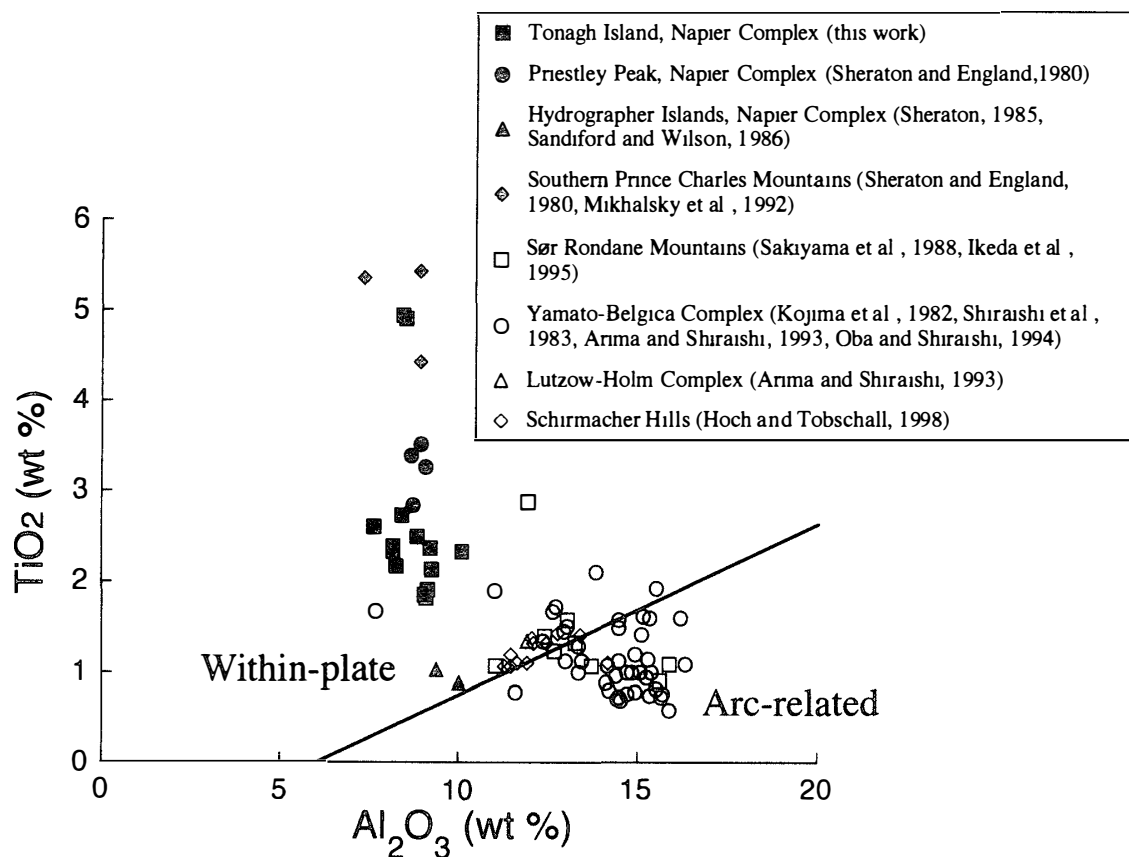


Fig 7 TiO_2 versus Al_2O_3 variation in lamproites from Enderby Land and the southern Prince Charles Mountains (solid symbols) and potassic to ultrapotassic igneous rocks from Eastern Queen Maud Land (open symbols). Line separates fields of within-plate and arc-related rocks (Muller *et al.*, 1992). Lamproites from Enderby Land plot in the within-plate field, whereas Queen Maud Land potassic to ultrapotassic rocks plot largely in the field of arc-related rocks, only a few plot in the within-plate field.

shallower emplacement (Sheraton and England, 1980)

A large number of potassic and ultrapotassic intrusions have been described from metamorphic and plutonic complexes west of Enderby Land in Eastern Queen Maud Land: the Schirmacher Hills, Sør Rondane Mountains, Yamato-Belgica Complex and Lützow-Holm Complex (Fig. 1) (Kojima *et al.*, 1982, Shiraishi *et al.*, 1983, Sakiyama *et al.*, 1988, Arima and Shiraishi, 1993, Oba and Shiraishi, 1994, Ikeda *et al.*, 1995, Hoch and Tobschall, 1998). Some of these potassic rocks have been metamorphosed under greenschist- or amphibolite-facies conditions, e.g., a metamorphosed ultrapotassic dyke giving a K-Ar whole-rock age of 434.6 ± 21.7 Ma at Innhovde, Lützow-Holm Bay (Arima and Shiraishi, 1993). The host rock at Innhovde, an orthogneiss, gave a 550 ± 12 Ma $^{206}Pb/^{238}U$ age as well as 900–1000 Ma $^{207}Pb/^{206}Pb$ ages using SHRIMP on zircon (Shiraishi *et al.*, 1992, 1994). These intrusions were regarded as products of post-orogenic magmatism originating from a mantle source after the peak of metamorphism (Arima and Shiraishi, 1993, Ikeda *et al.*, 1995). Arima and Shiraishi (1993) suggested that this late Neoproterozoic to Cambrian orogeny and associated magmatism, in Eastern Queen Maud Land, were related to the amalgamation of east and west Gondwana.

Overall, the temporal and spatial relationships between lamproite intrusion and zones of Cambrian reactivation of the Napier Complex are similar to those between ultrapotassic igneous activity and Pan-African deformation and metamorphism in Eastern Queen Maud Land. This suggests that the effects of the amalgamation of east and west Gondwana in Antarctica extended eastward to Enderby Land.

Acknowledgments

We express our sincere thanks to the members of JARE-40 and crew of the icebreaker "Shirase", especially Messrs Y Ohashi, K Maki, S. Harigai, T Takei and Dr H Yamuchi, who assisted in the helicopter operation. We also acknowledge the assistance of Ulrich Senff of the Australian National University in carrying out the chemical analyses of ESG's samples. Professors M Arima and H Kagami are acknowledged for critical reading of the manuscript. ESG's research was supported by U.S. National Science Foundation grant OPP-9813569 to the University of Maine.

References

- Arima, M and Shiraishi, K (1993) Geochemical characteristics of metamorphosed high K/Na dykes in eastern Queen Maud Land, Antarctica: ultrapotassic igneous activity linked to Pan-African orogeny. *Proc NIPR Symp Antarct Geosci*, **6**, 103-115
- Ben Othman, D, White, W M and Patchett, J (1989) The geochemistry of marine sediments, island arc magma genesis, and crust-mantle recycling. *Earth Planet Sci Lett*, **94**, 1-21
- Black, L P and James, P R (1983) Geological history of the Napier Complex of Enderby Land. *Antarctic Earth Science*, ed by R L Oliver *et al*. Canberra, Aust Acad Sci, 11-15
- Black, L P, James, P R and Harley, S L (1983) Geochronology and geological evolution of metamorphic rocks in the Field Islands area, East Antarctica. *J Metamorph Geol*, **1**, 277-303
- Black, L P, Harley, S L, Sun, S-S and McCulloch, M T (1987) The Rayner Complex of East Antarctica: complex isotopic systematics within a Proterozoic mobile belt. *J Metamorph Geol*, **5**, 1-26
- Deer, W A, Howie, R A and Zussman, J (1963) *Rock Forming Minerals*. 4 Framework Silicates, London, Longmans, 435 p
- Foley, S (1992) Petrological characterization of the source components of potassic magmas: geochemical and experimental constraints. *Lithos*, **28**, 187-204
- Foley, S F, Taylor, W R and Green, D H (1986) The role of fluorine and oxygen fugacity in the genesis of the ultrapotassic rocks. *Contrib Mineral Petrol*, **94**, 183-192
- Foley, S F, Ventturelli, G, Green, D H and Toscani, L (1987) The ultrapotassic rocks: Characteristics, classification and constraints for petrogenetic models. *Earth Sci Rev*, **24**, 81-134
- Grew, E S (1978) Precambrian basement at Molodezhnaya Station, East Antarctica. *Geol Soc Am Bull*, **89**, 801-813
- Grew, E S, Yates, M G, Belakovskiy, D I, Rouse, R C, Su, S-C and Marquez, N (1994) Hyalotekite from reedmergnerite-bearing alkali pegmatite, Dara-i-Pioz, Tajikistan and from Mn skarn, Långban, Värmland, Sweden: a new look at an old mineral. *Mineral Mag*, **58**, 285-297
- Grew, E S, Yates, M G, Barbier, J, Shearer, C K, Sheraton, J W, Shiraishi, K and Motoyoshi, Y (2000) Granulite-facies beryllium pegmatites in the Napier Complex in Khmara and Amundsen Bays, western Enderby Land, East Antarctica. *Polar Geosci*, **13**, 1-40
- Hanson, R E, Martin, M W, Bowring, S W and Munyanywa, H (1998) U-Pb zircon age from the Umkondo dolerites, eastern Zimbabwe: 1.1 Ga large igneous province in southern Africa-East Antarctica: possible Rodinia correlations. *Geology*, **26**, 1143-1146

- Harley, S L and Hensen, B J (1990) Archean and Proterozoic high-grade terrains of East Antarctica (40–80°E) a case study of diversity in granulite facies metamorphism High Temperature Metamorphism and Crustal Anatexis, ed by J R Ashworth and M Brown London, Unwin Hyman, 320–370 (Mineral Soc Ser, 2)
- Hoch, M and Tobschall, H J (1998) Minettes from Schirmacher Oasis, East Antarctica—indicators of an enriched mantle source *Antarct Sci*, **10**, 476–486
- Ikeda, Y, Shiraishi, K and Kagami, H (1995) Geochemical characteristics of mafic dike rocks from the Sør Rondane Mountains, East Antarctica *Proc NIPR Symp Antarct Geosci*, **8**, 49–64
- Ishizuka, H, Ishikawa, M, Hokada, T and Suzuki, S (1998) Geology of the Mt Ruser-Larsen area of the Napier Complex, East Antarctica *Polar Geosci*, **11**, 154–171
- Kamenev, E N (1972) Geological structure of Enderby Land Antarctic geology and geophysics—symposium on Antarctic geology and solid earth geophysics, Oslo, 6–15, August 1970, ed by R J Adie Oslo, Universitetsforlaget, 579–584
- Kamenev, E N (1975) The geology of Enderby Land Academy of Science of the USSR, Committee on Antarctica Research, Report No 14, 34–58 (In Russian)
- Kojima, H, Yanai, K and Nishida, T (1982) Geology of the Belgica Mountains *Mem Natl Inst Polar Res, Spec Issue*, **21**, 32–46
- Kononova, V A, Pervov, V A, Bogatkov, O A, Woolley, A and Saddebi, P (1997) Pseudoleucite and origin of highly potassic rocks of the southern Sakun Massif, Aldan Shield *Petrologiya*, **5**(2), 188–205 (in Russian)
- Mikhalsky, E V, Andronikov, A V and Beliatsky, B V (1992) Mafic igneous suites in the Lambert Rift Zone *Recent Progress in Antarctic Earth Science*, ed by Y Yoshida *et al* Tokyo, Terra Sci Publ, 173–178
- Mikhalsky, E V, Layba, A A, Beliatsky, B V, Sosedko, T A and Andronikov, A V (1994) Lamproites of Rubin Massif, Prince Charles Mountains, East Antarctica *Petrologiya*, **2**, 297–304 (in Russian)
- Miller, C, Schuster, R, Klotzli, U, Frank, W and Purtscheller, F (1999) Post-collisional potassic and ultrapotassic magmatism in SW Tibet Geochemical and Sr-Nd-Pb-O isotopic constraints for mantle source characteristics and petrogenesis *J Petrol*, **40**, 1399–1424
- Mitchell, R H and Bergman, S C (1991) *Petrology of Lamproites* New York, Plenum Press, 447 p
- Muller, D, Rock, N S M and Groves, D I (1992) Geochemical discrimination between shoshonitic and potassic volcanic rocks in different tectonic settings A pilot study *Mineral Petrol*, **46**, 259–289
- Oba, T and Shiraishi, K (1994) The emplacement pressure of syenite estimated from the stability field of amphibole from the Yamato Mountains, East Antarctica *Proc NIPR Symp Antarct Geosci*, **7**, 60–68
- Osanai, Y, Toyoshima, T, Owada, M, Tsunogae, T, Hokada, T and Crowe, W A (1999) Geology of ultrahigh-temperature metamorphic rocks from the Tonagh Island in the Napier Complex, East Antarctica *Polar Geosci*, **12**, 1–28
- Pognante, U (1990) Shoshonitic and ultrapotassic post-collisional dykes from northern Karakorum (Sinkiang, China) *Lithos*, **26**, 305–316
- Robert, U, Foden, J and Varne, R (1992) The Dodecanese Province, SE Aegean A model for tectonic control on potassic magmatism *Lithos*, **28**, 241–260
- Rock, N S M (1991) *Lamprophyres, with additional invited contributions by D R Bowes and A E Wright* Glasgow, Blackie and Son, 285 p
- Sakiyama, T, Takahashi, Y and Osanai, Y (1988) Geological and petrological characters of the plutonic rocks in the Lunckeryggen-Brattnipene region, Sør Rondane Mountains, East Antarctica *Proc NIPR Symp Antarct Geosci*, **2**, 80–95
- Sandiford, M and Wilson, C J L (1983) The geology of the Fyfe Hills-Khmara Bay region, Enderby Land *Antarctic Earth Science*, ed by R L Oliver *et al* Canberra, Aust Acad Sci, 16–19
- Sandiford, M and Wilson, C J L (1986) The origin of Archaean gneisses of the Fyfe Hills region, Enderby Land, field occurrence, petrography and geochemistry *Precambrian Res*, **31**, 37–

68

- Sheraton, J W (1985) Chemical analyses of rocks from East Antarctica Part 2 Bureau of Mineral Resources, Geology and Geophysics, Australia, Record 1985/12
- Sheraton, J and Black, L P (1981) Geochemistry and geochronology of Proterozoic tholeiite dykes of East Antarctica evidence for mantle metasomatism *Contrib Mineral Petrol*, **78**, 305-317
- Sheraton, J W and England, R N (1980) Highly potassic mafic dykes from Antarctica *J Geol Soc Aust*, **27**, 129-135
- Sheraton, J W, Offe, L A, Tingey, R J and Ellis, D J (1980) Enderby Land, Antarctica—an unusual Precambrian high grade metamorphic terrain *J Geol Soc Aust*, **27**, 1-18
- Sheraton, J W, Tingey, R J, Black, L P, Offe, L A and Ellis, D J (1987) Geology of Enderby Land and western Kemp Land, Antarctica *BMR Bull*, **223**, 51 p
- Shiraishi, K, Asami, M and Kanaya, H (1983) Petrochemical character of the syenitic rocks from the Yamato Mountains, East Antarctica *Mem Natl Inst Polar Res, Spec Issue*, **28**, 183-197
- Shiraishi, K, Hiroi, Y, Ellis, D J, Fanning, C N, Motoyoshi, Y and Nakai, Y (1992) The first report of a Cambrian orogenic belt in East Antarctica—An ion microprobe study of the Lutzow-Holm Complex *Recent Progress in Antarctic Earth Science*, ed by Y Yoshida *et al* Tokyo, Terra Sci Publ, 67-73
- Shiraishi, K, Ellis, D J, Hiroi, Y, Fanning, C N, Motoyoshi, Y and Nakai, Y (1994) Cambrian orogenic belt in East Antarctica and Sri Lanka Implications for Gondwana assembly *J Geol*, **102**, 47-65
- Smith, J V (1974) *Feldspar Minerals 2 Chemical and Textural Properties* New York, Springer Verlag, 690 p
- Steiger, R H and Jager, E (1977) Subcommittee on geochronology convention on the use of decay constants in geo- and cosmochronology *Earth Planet Sci Lett*, **36**, 359-362
- Sun, S-S and McDonough, W F (1989) Chemical and isotope systematics of oceanic basalts Implication for mantle composition and processes *Magmatism in the Ocean Basins*, ed by A D Saunders and M J Norry Oxford, Blackwell, 313-345
- Tainosho, Y, Kagami, H, Hamamoto, T and Takahashi, Y (1997) Preliminary result for the Nd and Sr isotope characteristics of the Archaean gneisses from Mount Pardoe, Napier Complex, East Antarctica *Proc NIPR Symp Antarct Geosci*, **10**, 92-101
- Taylor, S R and McLennan, S M (1985) *The Continental Crust Its Composition and Evolution* Oxford, Blackwells Scientific, 312 p
- Thompson, R N and Fowler, M B (1986) Subduction-related shoshonitic and ultrapotassic magmatism a study of Siluro-Ordovician syenites from the Scottish Caledonides *Contrib Mineral Petrol*, **94**, 507-522
- Vaselli, O and Conticelli, S (1990) Boron, cesium and lithium distribution in some alkaline potassic volcanics from Central Italy *Mineral Petrogr Acta*, **33**, 189-204
- Williams, I S, Compston, W, Black, L P, Ireland, T R and Foster, J J (1984) Unsupported radiogenic Pb in zircon a cause of anomalously high Pb-Pb, U-Pb, and Th-Pb ages *Contrib Mineral Petrol*, **88**, 322-327
- Woolley, A R, Bergman, S C, Edgar, A D, Le Bas, M J, Mitchell, R H, Rock, N M S and Scott Smith, B H (1996) Classification of lamprophyres, lamproites, kimberlites, and the kalsilitic, melilitic, and leucitic rocks *Canad Mineral*, **34**, 175-186
- Yanagi, T (1990) A new method for accurate determination of isotope composition and concentration of strontium in a spike solution used for geochronology works *Mass Spectrosc*, **38**, 193-198
- Yanagi, T, Baadsgaard, H, Stelck, C R and McDougall, I (1988) Radiogenic dating of a tuff bed in the middle Albein Hulcross Formation at Hudson's Hope, British Columbia *Can J Earth Sci*, **25**, 1123-1127
- York, D (1966) Least-squares fitting of a straight line *Can J Phys*, **44**, 1079-1086

(Received January 28, 2000, Revised manuscript accepted March 24, 2000)